# Structure−Function Correlations of the Reaction of Reduced Nicotinamide Analogues with *p*-Hydroxybenzoate Hydroxylase Substituted with a Series of 8-Substituted Flavins†

Mariliz Ortiz-Maldonado, Domenico Gatti,‡ David P. Ballou,* and Vincent Massey*

*Department of Biological Chemistry, University of Michigan, Ann Arbor, Michigan 48109-0606, and Department of Biochemistry and Molecular Biology, Wayne State University, Detroit, Michigan 48201*

*Received July 12, 1999; Revised Manuscript Received October 5, 1999*

ABSTRACT: Structural and kinetic studies have revealed two flavin conformations in *p*-hydroxybenzoate hydroxylase (PHBH), the in-position and the out-position. Conversion between these two conformations is believed to be essential during catalysis. Although substrate hydroxylation occurs while the flavin in PHBH is in the in-conformation, the position of the flavin during reduction by NADPH is uncertain. To investigate the catalytic importance of the out-conformation of the flavin and to clarify the mechanism of flavin reduction in PHBH, we report quantitative structure−reactivity relationships (QSAR) using PHBH substituted separately with nine derivatives of FAD modified in the 8-position and four dihydronicotinamide analogues as reducing agents. The 8-position of the FAD isoalloxazine ring was chosen for modification because in PHBH it has minimal interactions with the protein and is accessible to solvent. The chemical sequence of events during catalysis by PHBH was not altered when using any of the modified flavins, and normal products were obtained. Although the rate of reduction of PHBH reconstituted with flavin derivatives is expected to be dependent on the redox potential of the flavin, no strict correlation was observed. Instead, the rate of reduction correlated with the $\kappa$-substituent constant, which is based on size and hydrophobicity of the 8-substituent on the FAD. Substituents that sterically hinder attainment of the out-conformation decreased the rate of flavin reduction much more than expected on the basis of the redox potential of the flavin. The results of this QSAR analysis are consistent with the hypothesis that the flavin in PHBH must move to the out-conformation for proper formation of the charge-transfer complex between NADPH and FAD that is necessary for rapid flavin reduction.

Enzymes encounter a variety of conformational changes in solution and during catalysis; however, determining how protein dynamics contributes to catalysis is difficult. X-ray crystallography has been useful in helping to determine the roles of active-site residues in catalysis. In addition, it has shown in some cases that ligand binding induces significant changes in protein conformation. For example, active sites of enzymes often have an open conformation that provides access to ligands. Upon ligand binding, some proteins adopt a closed conformation to sequester the ligand from solvent and to align important amino acid residues for efficient catalytic turnover. Such closed conformations can also prevent reactive intermediates from being discharged during catalysis. In ligand-free enzyme, movement between open and closed conformations presumably can also occur, but the equilibrium usually lies toward the open structure. Motions between conformations may constitute important steps during catalysis, and these motions can be as large as domain movements or as small as fluctuations of side chains. Conformational changes in some cases are the rate-limiting steps during catalysis. For example, the rate-limiting step in both phosphoglycerate kinase (*1*, *2*) and in hexokinase (*3*) is the dissociation of product, and this step is believed to be limited by a conformational change from the closed to the open conformation.

The flavoprotein *p*-hydroxybenzoate hydroxylase (PHBH,[1,2] EC 1.14.13.2) is one of the bacterial enzymes directly involved in soil bioremediation. PHBH catalyzes the NADPH- and oxygen-dependent hydroxylation of *p*-hydroxybenzoate (*p*-OHB) (Scheme 1), an important step in the degradation of many aromatic compounds. Wild-type and site-directed mutant forms of PHBH from the bacterial strain *Pseudomonas* have been extensively studied by transient-state kinetics (*4*−*13*) and protein crystallography (*9*, *14*−*16*). The X-ray structures of wild-type and mutant forms of

† Financial support was received from United States Public Health Service (GM 20877 to D.P.B., GM 11106 to V.M.) and The University of Michigan Rackham Merit Fellowship (to M.O.-M.).

* To whom correspondence should be addressed. (D.P.B.) University of Michigan. E-mail: dballou@umich.edu. Phone: (734) 764-9582. Fax: (734) 763-4581. (V.M.) University of Michigan. E-mail: massey@umich.edu. Phone: (734) 764-7196. Fax: (734) 763-4581.

‡ Wayne State University.

[1] Abbreviations: PHBH, *p*-hydroxybenzoate hydroxylase from *Pseudomonas aeruginosa*; *p*-OHB, *p*-hydroxybenzoate; 2,4-DOHB, 2,4-dihydroxybenzoate; 3,4-DOHB, 3,4-dihydroxybenzoate; FAD, flavin adenine dinucleotide; ApoPHBH, the apoenzyme form of *p*-hydroxybenzoate hydroxylase; $FADH^-$, reduced flavin adenine dinucleotide; NADH, reduced nicotinamide adenine dinucleotide; NADPH, reduced nicotinamide adenine dinucleotide phosphate; NMNH, reduced nicotinamide mononucleotide; NMeH, reduced *N*-methylnicotinamide; $NMe^+Cl^-$, oxidized *N*-methylnicotinamide salt; $P_i$, phosphate; QSAR, quantitative structure−activity relationship; $E^{o\prime}$, redox potential at pH 7.0; $\kappa$, charge-transfer substituent constant; *R*, regression value from the curve fit; *F*, statistical F.

[2] The PDB accession number for the structure of PHBH reconstituted with 8-$N(CH_3)_2$-FAD is 1D7L.

10.1021/bi991603u CCC: $18.00 
Published on Web 11/19/1999

Scheme 1

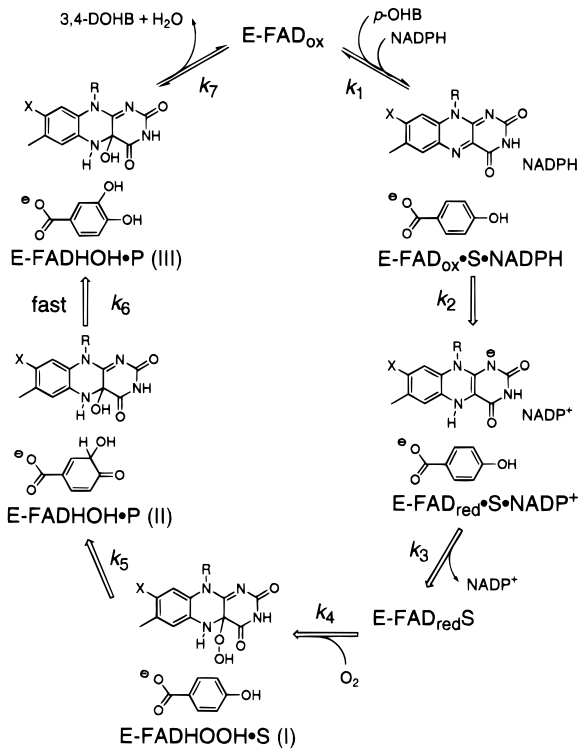


PHBH in the presence of different ligands have contributed significantly to the identification of active-site residues participating in catalysis. Moreover, these studies have indicated that the flavin prosthetic group can occupy two positions on the enzyme (Figure 1), depending on which ligand is bound or which active-site residue is changed (*14*, *15*). Motions between these two flavin conformations are essential during catalysis. There is strong evidence that the out-conformation—where the isoalloxazine ring of the flavin swings out about 45° along the dihedral angle defined by C1′, C2′, and C3′ of the FAD and is exposed to solvent—is essential for substrate-binding dynamics (*14*) and for reduction of the FAD by NADPH (*17*, *18*). The crystal structure of PHBH (*14*, *15*, *19*) suggests strongly that the flavin must be in the in-conformation for the hydroxylation reaction to occur. The in-conformation of the flavin sequesters the reactive flavin-C4a-hydroperoxide intermediate from solvent to prevent the unwanted elimination of $H_2O_2$. The crystal structure of phenol hydroxylase, a flavoprotein monooxygenase from the same family as PHBH, also presents two flavin conformations in the active site (open and closed) (*20*). It has been suggested that these conformations are similarly involved during catalysis by phenol hydroxylase and perhaps in several members of this family of enzymes.

Unfortunately, no crystal structure of PHBH with NADPH bound has yet been determined, so that the position of the flavin in PHBH during the reduction step is unknown. Studies with enzymes in which the native FAD has been replaced by 8-hydroxy-5-deaza-FAD have shown that in all members of the flavoprotein hydroxylase family studied, pyridine nucleotide interaction is with the *re*-face of the flavin (*21*). Moreover, it has been shown that the pro-R hydrogen of the nicotinamide ring of NADPH is stereospecifically transferred (*22*) to the *re*-face of the isoalloxazine ring of the flavin (*21*). A primary deuterium isotope effect of 10 is observed during reduction of the flavin by NADPD (*18*, *22*). Thus, the facial disposition of the flavin and the nicotinamide rings during hydride transfer is well-defined. No direct evidence about the position of the flavin during reaction with NADPH is available. However, kinetic, crystallographic, and modeling studies of WT and two mutant forms of PHBH clearly show that pyridine nucleotide binding consistent with the known stereospecific hydride transfer is possible only with the flavin in the out-position (*23*).

To further investigate the role(s) for these dynamic motions in PHBH during the reductive half reaction, we studied the effects of nine 8-substituted flavins (the 8-position is accessible to solvent in either conformation) and of four dihydronicotinamide analogues on the hydride-transfer reaction. The importance of active-site dynamics during catalysis is demonstrated by this kinetic analysis of enzymes modified by cofactor substitution. Our studies provide further evidence that flavin movement is required in the reduction of FAD by NADPH.

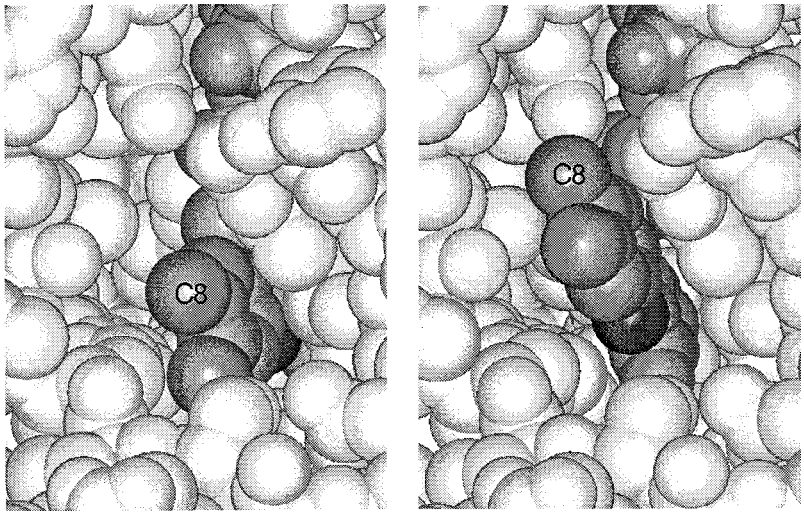


FIGURE 1: Flavin conformations in PHBH. The 8-position of the flavin is accessible to solvent when the conformation of the FAD is in (left) or out (right). The flavin is shaded in gray, with N5 in dark gray. The *si*-side of the flavin is to the right of the viewer and the *re*-side, where hydride transfer from NADPH occurs, is on the left and partly obscured. The nicotinamide presumably binds in the pocket on the flavin *re*-face. Such a pocket is not available with the flavin in the in-position.

## EXPERIMENTAL PROCEDURES

*Materials*. Substituted riboflavin analogues were obtained from various sources or synthesized as previously described (*24*). The conversion of riboflavin analogues into the corresponding FAD analogue was achieved using FAD synthetase and flavokinase isolated from *Brevibacterium ammoniagenes* as reported in ref *25*. The extinction coefficients used for the various free 8-substituted FAD analogues ($M^{-1}$ $cm^{-1}$) were $\epsilon_{448}$ (Cl) = 10 600, $\epsilon_{450}$ (H) = 11 300, $\epsilon_{450}$ (CN) = 11 400, $\epsilon_{450}$ ($CH_3$) = 11 300, $\epsilon_{474}$ ($SCH_3$) = 28 500, $\epsilon_{482}$ ($NH_2$) = 44 000, $\epsilon_{486}$ (hydroxy) = 32 200, $\epsilon_{505}$ [$N(CH_3)_2$] = 32 800, and $\epsilon_{534}$ (mercapto) = 30 000.

The highest purity NADPH, NADH, NMNH, $NMe^+Cl^-$, and $Na_2S_2O_4$ were used as purchased from Sigma, while *p*-OHB and 2,4-DOHB were recrystallized before use. All other chemicals were described elsewhere (*24*). The concentrations of the following solutions were as estimated spectrophotometrically using $\epsilon_{340}$ = 6220 $M^{-1}$ $cm^{-1}$ for NADPH, NADH, and NMNH, $\epsilon_{265}$ = 3940 $M^{-1}$ $cm^{-1}$ for $NMe^+$, $\epsilon_{360}$ = 7060 $M^{-1}$ $cm^{-1}$ for NMeH, $\epsilon_{292}$ = 9000 $M^{-1}$ $cm^{-1}$ for 2,4-DOHB (in 1 N HCl) and $\epsilon_{282}$ = 16 300 $M^{-1}$ $cm^{-1}$ for *p*-OHB (in 1 N NaOH).

*PHBH Purification and Apoenzyme Preparation.* PHBH was expressed and purified from extracts of *E. coli* JM105/pIE-130 using published procedures (*26*). ApoPHBH was prepared as reported by Müller et al. (*27*), but with the modifications reported in ref *24*, implemented to increase the yield of apoenzyme. The purified apoenzyme had no detectable activity in assay mixtures lacking FAD and no absorbance at wavelengths greater than 310 nm. The molar absorptivity at 280 nm of apoPHBH used was 73 000 $M^{-1}$ $cm^{-1}$ (*24*).

*PHBH with 8-Substituted FAD Forms.* ApoPHBH in 0.1 M Tris-sulfate buffer (pH 8.0) containing 1 mM EDTA was reconstituted by incubating it for 1 h at 25 °C with a 1.5−2-fold molar excess of 8-substituted-FAD as reported in ref *24*. Each 8-substituted FAD binds tightly to PHBH as evidenced by the lack of flavin dissociation from the enzyme during gel-filtration or ultrafiltration. The methods for determining extinction coefficients for the various types of oxidized 8-substituted-FAD PHBH, as well as the enzymatic hydroxylation and the dissociation constants for *p*-OHB and 2,4-DOHB, have been described in detail (*26*) and reported in ref *24*. The redox potentials of PHBH reconstituted with the 8-substituted flavins, in the presence or absence of *p*-OHB, were determined as described in ref *28* and are reported in ref *24*.

*Crystallization, Data Collection, and Structure Refinement of PHBH Reconstituted with 8-N($CH_3$)$_2$-FAD.* Orthorhombic crystals (space group $C222_1$) of *P. aeruginosa* PHBH reconstituted with 8-N($CH_3$)$_2$-FAD were grown at pH 7.4 in the presence of 2 mM *p*-OHB and 0.040 mM 8-N($CH_3$)$_2$-FAD by free interface diffusion in sealed melting point capillaries as described by van der Laan et al. (*29*). For data collection, a single crystal was flash-frozen at 100 K in a cryo-protectant solution consisting of 0.1 M potassium phosphate (pH 7.4), 60% saturated ammonium sulfate, 15% glycerol, 0.020 mM 8-N($CH_3$)$_2$-FAD, 0.1 mM glutathione, and 1 mM *p*-OHB. Diffraction data were collected at 100 K with a dual multiwire area detector (ADS, San Diego, CA). Data reduction and scaling were performed with ADS software. The structure of the native *P. aeruginosa* enzyme (*10*) was used as the starting model for the refinement of the structure of the enzyme reconstituted with 8-N($CH_3$)$_2$-FAD. The refinement was performed with CNS (*30*) and included all reflections between 40 and 2.2 Å without $\sigma$ cutoff and with calculation of a bulk solvent mask. Cross-validated Maximum Likelihood (*31*) was used as the target function. Model coordinates were adjusted to the new unit cell by rigid body minimization of the three domains of the enzyme, the 8-N($CH_3$)$_2$-FAD, and the substrate. Positional parameters were then optimized by torsional dynamics using the slow-cool protocol in the range 1000−300 K. Solvents were added using the CNS automated procedure that takes into account both crystallographic and chemical criteria and checked interactively using the graphic visualization and modeling program XtalView (*32*). Positional and thermal parameters were refined iteratively after each round of solvent addition. The X-ray diffraction data and refinement statistics are summarized in Table 1.

Table 1: Data Set and Crystallographic Refinement Statistics of PHBH Reconstituted With 8-N($CH_3$)$_2$-FAD Complexed with *p*-OHB

| parameter | value | parameter | value |
|---|---|---|---|
| *a* axis (Å) | 70.802 | $R_{sym}$ (high res)[a] | 0.28 |
| *b* axis (Å) | 145.477 | $R_{cryst}$[c] (free R) | 0.191 (0.241) |
| *c* axis (Å) | 86.966 | solvent content (%) | 56.5 |
| resolution (Å) | 40-2.2 | solvents | 244 |
| unique reflections | 22994 | RMS coord error[d] (Å) | 0.25 |
| completeness (%) | 98.9 | RMS deviations[d] | |
| ⟨redundancy⟩ | 3.9 | bond length (Å) | 0.007 |
| $\langle I/\sigma I\rangle$ | 6.27 | angles (deg) | 1.339 |
| $\langle I/\sigma I\rangle$ (High Res)[a] | 1.83 | dihedrals (deg) | 22.736 |
| $R_{sym}$[b] | 0.13 | impropers (deg) | 0.869 |

[a] High resolution shell: 2.200−2.213 Å. [b] $R_{sym} = \sum(h)\sum(i)|I(h,i) - \langle I(h)\rangle|/\sum(h)\langle I(h)\rangle$ [where $\langle I(h)\rangle$ = mean intensity of symmetry equivalent reflections]. [c] $R_{cryst} = \sum(h)||F_{obs}(h)| - k|F_{calc}(h)||/\sum(h)|F_{obs}(h)|$. [d] RMS coordinate error and RMS deviations from ideality for bonds and angles were calculated with CNS (*30*).

*Synthesis of N-Methyl-dihydronicotinamide.* Reduced *N*-methyl nicotinamide was synthesized using the procedure reported in ref *33* for the synthesis of *N*-propyl-dihydronicotinamide. *N*-Methyl nicotinamide chloride ($NMe^+Cl^-$) (0.2 g) was dissolved in 6 mL of HPLC-grade water in a 25 mL round-bottomed flask and made alkaline by the addition of 0.85 g of anhydrous $Na_2CO_3$. The pale yellow solution was placed on an ice bath, and 0.85 g of $Na_2S_2O_4$ was added in small portions over 1 min while an argon flow over the surface of the solution was applied. Once all the $Na_2S_2O_4$ was added, the flask was capped with a septum and an argon flow was passed through; the dark orange solution was stirred under argon for 2 h to remove $SO_2$; the solution turned to a bright yellow color and a white precipitate was observed.

Once the reaction was completed, *N*-methyl-dihydronicotinamide (NMeH) was extracted three times with 25 mL of chloroform and dried using a rotary evaporator under vacuum. The oily yellow product was stored under argon at −20 °C until used. Crystallization of the product using ether or methanol was not successful because the compound decomposes rapidly at room temperature. NMeH is reasonably stable in 0.1 M Tris-sulfate buffer (pH 8.0), whereas its decomposition is evident in KPi buffer, pH 6.5. NMeH was obtained in 65% overall yield based on extinction changes. Mass spectrometry (in water) and $^1H$ NMR (500 MHz, in $D_2O$) data for the NMeH product showed the

Scheme 2

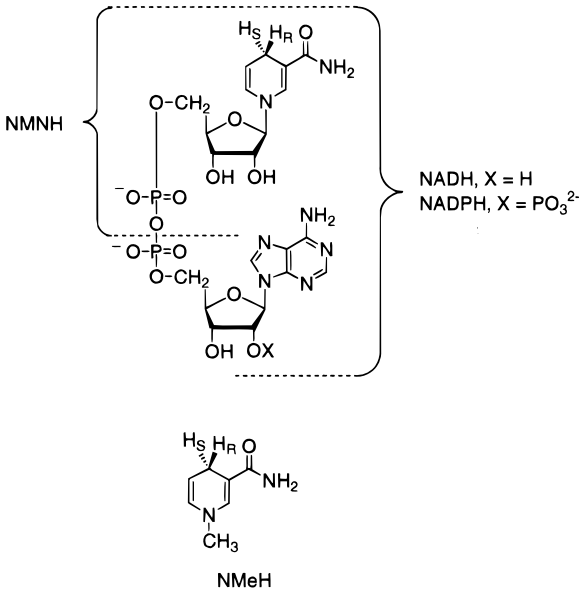


expected signals (data not shown). Product decomposition in aqueous solution at low pH can be detected by the increase in absorbance at 290−300 nm and the decrease at 360 nm. NMeH used in these experiments was freshly prepared in 10 mM Tris-$SO_4$.

*Transient State Kinetics*. The instruments used during transient-state kinetics experiments were described in ref *24*. The stopped-flow apparatus was made anaerobic by using the protocatechuic acid (PCA)/protocatechuic acid dioxygenase (PCD) system as described in ref *24*. Reduction reactions and measurements were carried out at 4 °C in 50 mM $KP_i$ buffer (pH 6.5) or 100 mM Tris-sulfate buffer (pH 8.0). Enzyme (30 $\mu$M) (in the presence of 0.5−1.0 mM *p*-OHB) in a glass tonometer was made anaerobic by repeated cycles of evacuation and equilibration with purified argon. The reduction of oxidized enzyme under anaerobic conditions was initiated by mixing enzyme with buffered solutions containing various concentrations of NADPH, NADH, NMNH, or NMeH (Scheme 2). Rate constants were calculated from exponential fits of absorbance traces recorded at appropriate wavelengths, using the programs KISS and Program A, which use the Marquardt algorithm (*34*). The concentration of the nicotinamide analogues used in these experiments varied depending on the dissociation constant obtained from the kinetics of reduction.

## RESULTS

*Spectral Properties of PHBH Reconstituted with 8-Substituted FAD Analogues.* Substitution at the 8-position of the FAD by groups with varied electronic properties alter the UV−vis absorbance spectrum of the flavin. Spectra for the PHBH-bound flavin analogues used in this study, both in oxidized and reduced states, are shown in Figure 2. The 8-position of the flavin is insulated from the redox center of the molecule (N1, C10a, C4a, and N5) by five atoms; therefore, the effects conferred to the flavin by 8-substituents are mainly inductive. Flavin analogues substituted at the 8-position with basal (−H) or electron-withdrawing groups such as −Cl or −CN have spectra that are similar to those of normal FAD (Figure 2, left column). These substituents increase the redox potentials of both the *free* and the enzyme-bound flavins (Table 2 and ref *24*). Other flavin analogues containing electron-donating groups at the 8-position such as $-SCH_3$, $-N(CH_3)_2$, −mercapto, $-NH_2$, and -hydroxy have UV−vis absorbance properties that are different from those of native FAD (Figure 2). Most of these substituents decrease the redox potential of both *free* and enzyme-bound flavin (Table 2 and ref *24*).

*Structural Properties of PHBH Reconstituted with 8-N-$(CH_3)_2$-FAD*. The overall structure of PHBH reconstituted with 8-$N(CH_3)_2$-FAD is very similar to that of the native enzyme. The flavin occupies the in-position with its 8-dimethyl-amino moiety protruding toward the solvent (Figure 3). The planar 8-$N(CH_3)_2$ group is tilted by approximately 35° with respect to the plane of the isoalloxazine ring. A sulfate ion is bound near the 8-$N(CH_3)_2$ group, stabilized by a salt bridge to the guanidinium moiety of Arg44. Two other sulfate ions were identified in this structure. One is located in an anion hole formed by the side chains of Arg63, Arg64, and Arg67. The other is stabilized by salt bridges to the guanidinium groups of Arg327 and Arg334. The positions of the three sulfate ions identified in the structure of 8-$N(CH_3)_2$-FAD-substituted PHBH are occupied by solvent molecules in the structure of native PHBH. Only very small differences with respect to the structures of the native enzyme at pH 5.0, 7.4, and 9.4 (*10*) are observed in the vicinity of the substrate *p*-OHB and of several amino acid side chains that participate in the architecture of the active site. These are summarized in Table 3.

Under conditions in which the substrate is deprotonated (for example at pH 9.4), there is a repulsive interaction between the negatively charged O4 of the substrate and the carbonyl of Pro293, and the distance between these atoms increases (*10*). The particularly short distance (2.74 Å) between the substrate O4 and the carbonyl oxygen of Pro293 observed in the structure of 8-$N(CH_3)_2$-FAD-substituted PHBH suggests that the substrate *p*-OHB is protonated in this form of the enzyme. This observation is consistent with the biochemical data (data not shown; $pK_a$ value was determined according to ref *26*), indicating that the $pK_a$ of the substrate is ≥8.5 in the 8-$N(CH_3)_2$-FAD enzyme.

*Substrate Binding.* Flavins substituted at the 8-position were selected for this study because the 8-position of the flavin is solvent accessible (*36*) and distant from the binding site of *p*-OHB (*9*, *13*−*16*) (Figure 1); therefore, modification at the 8-position of the FAD is not expected to significantly affect substrate binding. The flavin in PHBH can be found either buried in the active site (in-conformation) or more accessible to solvent (out-conformation) (Figure 1), depending on the type of ligand bound to the enzyme or single amino acid replacement in the active site. Ligand binding to oxidized PHBH has been shown to drive the equilibrium of flavin movement to either the in-conformation (*p*-OHB) or the out-conformation (2,4-DOHB) (*14*). The conformation of the flavin can be detected either by distinctive changes in the absorbance spectrum upon substrate binding or by the determination of the protein crystal structure. Spectral perturbations for the titration of *p*-OHB and 2,4-DOHB to some of the modified enzymes are shown in Figure 4.

When PHBH is reconstituted with 8-Cl-FAD, 8-H-FAD, and 8-CN-FAD, flavin analogues that in the oxidized form are spectrally similar to FAD, the enzyme spectrum is

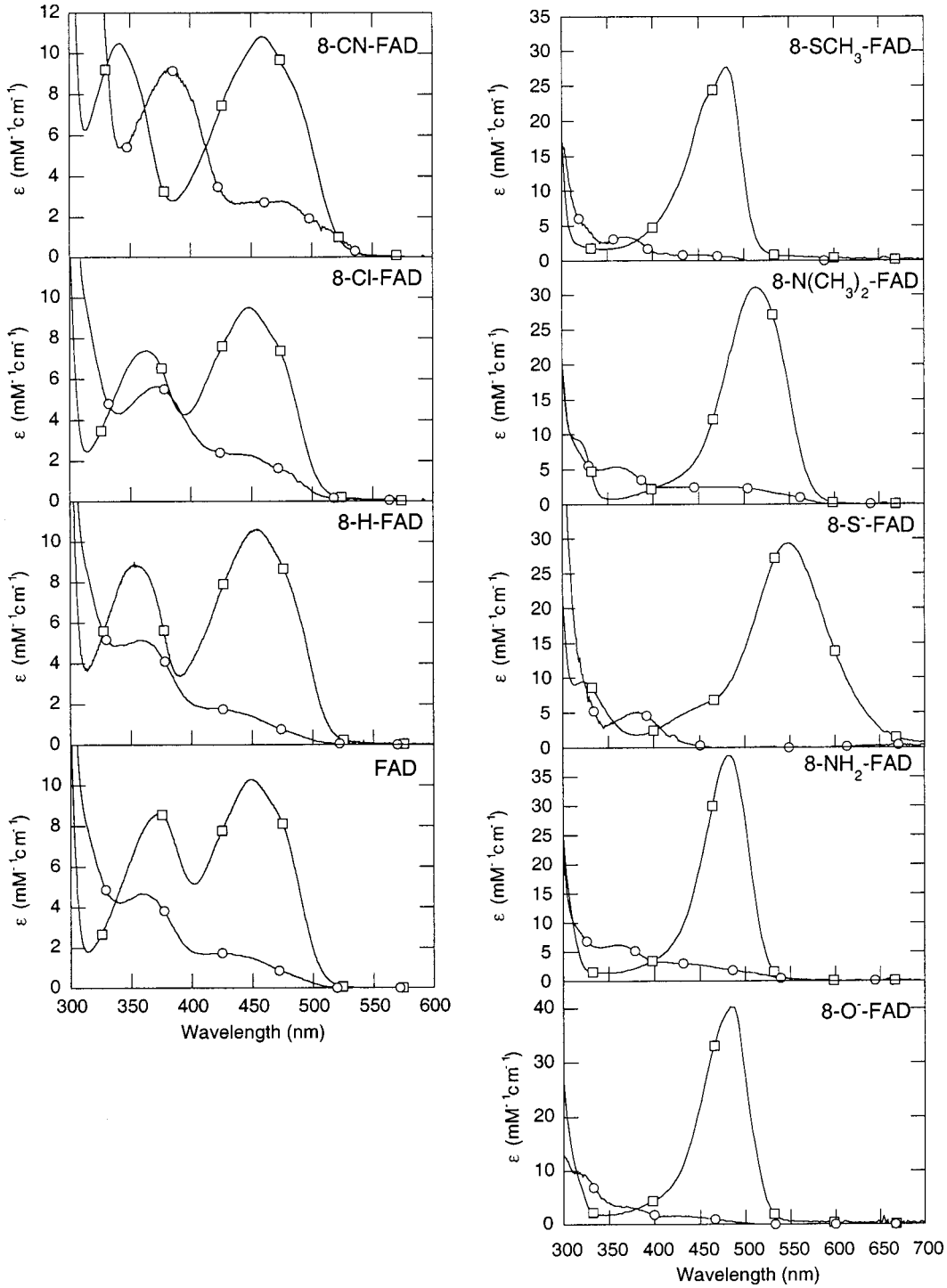


FIGURE 2: Spectra of the enzyme-bound flavin analogues. Spectra were recorded in 50 mM $KP_i$ buffer (pH 6.5) at 25 °C. Oxidized (□) form of the enzyme-bound flavins. The reduced (○) state of the enzyme was achieved by titration with dithionite, by using the glucose-6-phosphate/glucose-6-phosphate dehydrogenase generating system or by using the xanthine/xanthine oxidase method as reported in (*24*).

perturbed upon *p*-OHB binding similarly to that for enzyme containing FAD. This type of perturbation corresponds to the movement of the flavin toward the in-conformation (Figure 4, panels A and B). Binding of 2,4-DOHB to PHBH reconstituted with these three flavin analogues causes spectral perturbations consistent with the flavin moving away from the active site as observed previously in native PHBH (*14*), see below.

Assignment of the flavin position in PHBH-containing flavins with unusual UV−vis absorbance properties (Figure 2) by spectral changes alone is not clear. Crystallographic evidence shows that *p*-OHB binding to PHBH reconstituted with 8-$N(CH_3)_2$-FAD, the largest substituent used in this study, maintains the flavin buried in the active site (in-conformation). Although this enzyme variant in complex with 2,4-DOHB did not give good crystals for the determination of the molecular structure, binding of 2,4-DOHB shows spectral perturbations that are clearly different than those observed for *p*-OHB binding to this enzyme (Figure 4D). Binding of either *p*-OHB or 2,4-DOHB to enzyme substituted with flavin analogues with unusual UV−vis absorbance properties gave distinct spectral perturbations, suggesting

Table 2: Thermodynamic and Kinetic Constants of PHBH Reconstituted with 8-Substituted Flavins

| | | | $K_d$ ($\mu$M) | | | | | $k_2$ ($s^{-1}$)[a] | | |
|---|---|---|---|---|---|---|---|---|---|---|
| | | | pH 6.5 | | | pH 8.0 | | pH 6.5 | pH 8.0 | |
| | 8-substituent | $E^{\circ\prime}$ (mV)[b] | *p*-OHB[b] | 2,4DOHB[c] | NADPH[d] | NADPH[d] | NMeH[d] | NADPH | NADPH | NMeH |
| 1 | CN | +60 | 100 | 44 | 408 | 247 | 520 | 27.8 | 85.7 | 44 |
| 2 | Cl | −81 | 30 | 43 | 400 | 220 | 540 | 80 | 312 | 35.4 |
| 3 | H | −151 | 81 | 42 | 640 | 410 | 810 | 53 | 192 | 17.6 |
| 4 | $SCH_3$ | −152 | 19 | 76 | 399 | 300 | 2500 | 1.3 | 20.8 | 3.24 |
| 5 | $CH_3$ | −165[e] | 9.5[e] | 22 | 210 | 68 | 810 | 52 | 94 | 13.3 |
| 6 | $N(CH_3)_2$ | −210 | 17 | >500[f] | 5500[g] | 3600[g] | 1030 | 0.0014[g] | 0.023[g] | 0.25 |
| 7 | $S^-$ | −267 | 16 | ≤280[h] | 1500 | nd[i] | nd[i] | 0.026 | nd[i] | nd[i] |
| 8 | $NH_2$ | −298 | 31 | nd[i] | 62 | 18 | 1140 | 0.044 | 0.067 | 0.021 |
| 9 | $O^-$ | −308 | 31 | nd[i] | 1170 | nd[i] | nd[i] | 0.048 | nd[i] | nd[i] |

[a] Reduction rate constants were determined in solutions containing p-OHB either in 50 mM KPi buffer (pH 6.5) or 100 mM Tris-sulfate buffer (pH 8.0) at 4 °C, unless otherwise noted. Values of rate constants were the average of at least four determinations. Rate constants varied ≤5% from one another. [b] Values taken from ref *24*. [c] Dissociation constants for 2,4DOHB were determined from titrations in 50 mM $KP_i$ buffer (pH 6.5) at 4 °C. Individual measurements for the given flavin varied ≤5 $\mu$M. [d] Dissociation constants for nicotinamide analogs were calculated from the kinetics of reduction of enzyme complexed with *p*-OHB determined in 50 mM $KP_i$ buffer (pH 6.5) and 100 mM Tris-sulfate buffer (pH 8.0) at 4 °C, unless otherwise noted. Individual measurements for the given flavin varied ≤5 $\mu$M. The mechanism of reduction of enzyme by the nicotinamide analogs is represented in Scheme 1. [e] Value taken from ref *26*. [f] 500 $\mu$M did not saturate the enzyme. [g] Value determined at 25 °C. [h] Dissociation constant was determined kinetically from titrations in 50 $\mu$M $KP_i$ buffer (pH 6.5) at 4 °C using a stopped-flow spectrophotometer. Values of rate constants were the average of at least four determinations. Rate constants varied ≤5% from one another. [i] nd = not determined.

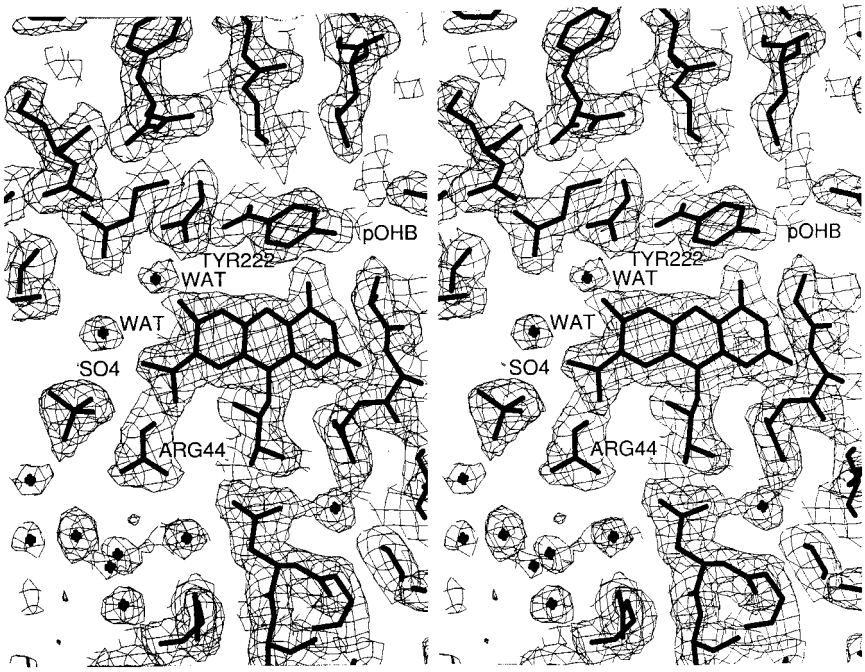


FIGURE 3: Stereoview of the active site of 8-$N(CH_3)_2$-FAD substituted PHBH. A Sigmaa (*44*) weighted $|2F_o - F_c|$ electron density map of the enzyme is contoured at 1$\sigma$ above the mean. The substituted flavin is shown from its *re*-side. A sulfate ion, stabilized by a salt bridge to Arg 44, is located in proximity of the C8 dimethyl-amino substituent of the flavin. The substrate (*p*-OHB), Tyr222, and two water molecules (WAT) are clearly visible. This figure was prepared using the program XtalView (*35*).

different flavin positions in the active site. Previously, it has been shown that PHBH reconstituted with 8-substituted flavins all bind *p*-OHB normally ($K_d$ = 10−100 $\mu$M) and are nearly fully coupled to form 87−100% of normal product, 3,4-DOHB (*24*). Thus, the flavin analogues used can move into the in-position where hydroxylation takes place. PHBH substituted with 8-CN-, 8-Cl-, 8-H-, 8-$SCH_3$- and 8-mercapto-FAD all bind the substrate analogue 2,4-DOHB normally ($K_d$ = 22−280 $\mu$M), whereas binding of 2,4-DOHB to enzyme reconstituted with the largest flavin analogue, 8-$N(CH_3)_2$-FAD, is impaired ($K_d$ > 500 $\mu$M) (Table 2).

*Reductive Half-Reaction of PHBH Variants by NADPH.* The oxidized form of PHBH reconstituted with 8-substituted-FAD analogues was mixed anaerobically with NADPH in the presence of a saturating concentration of *p*-OHB (0.5−1.0 mM) at pH 6.5 or 8.0 (see Experimental Procedures). The mechanism of flavin reduction was the same for all of the 8-substituted flavins in PHBH (as described below), but[4] the rate constants of steps during the reductive half reaction varied depending on the flavin analogue bound to PHBH.

The reaction of NADPH with the flavin-substituted enzymes initially forms a ternary complex between the enzymes and NADPH. This step of the reductive half reaction in most cases occurs very fast (≥$10^6$ $M^{-1}$ $s^{-1}$) with half-lives shorter than the dead time of the stopped-flow instrument. Upon forming the complex, the initial absorbance at $\lambda_{max}$ for the enzyme-bound flavins decreases slightly, and

Table 3: Distances (Å) between Selected Atoms in the Structures of Native PHBH at pH 5.0, 7.4, and 9.4, and 8-N$(CH_3)_2$-FAD Substituted PHBH at pH 7.4

| | native PHBH[a] | | | 8-N$(CH_3)_2$-FAD substituted PHBH |
|---|---|---|---|---|
| pH | 5.0 | 7.4 | 9.4 | 7.4 |
| sub O1*-Arg214 NH1 | 2.68 | 2.83 | 2.83 | 2.89 |
| sub O2*-Arg214 NH2 | 2.79 | 2.81 | 2.84 | 2.93 |
| sub O1*-Tyr222 OH | 2.58 | 2.62 | 2.61 | 2.52 |
| sub O2*-Ser212 OG | 2.77 | 2.70 | 2.67 | 2.65 |
| sub O4-Pro293 OH | 2.85 | 2.83 | 3.26 | 2.74 |
| sub O4-Tyr201 OH | 2.61 | 2.80 | 2.69 | 2.71 |
| Tyr201 OH-Tyr385 OH | 2.79 | 2.85 | 2.68 | 2.67 |

[a] Distances are from ref *10*.

the change in absorbance is dependent on the concentration of NADPH. It is also more pronounced in reactions at high pH. This step represents the formation of a charge-transfer complex between NADPH and oxidized flavin (*18*). Enzyme reconstituted with 8-$SCH_3$-FAD is the only example that shows a small increase in absorbance at its UV−vis absorbance maximum (483 nm) at pH 8.0 (Figure 5) before 10 ms. The formation of the NADPH·oxidized flavin charge-transfer complex ($\sim 2.7 \times 10^5$ $M^{-1}$ $s^{-1}$) can also be detected at 550 nm by an increase in absorbance (Figure 5).

After the formation of the initial charge-transfer complex, hydride transfer occurs from NADPH to the flavin. For most of the flavin analogues, traces at $\lambda_{max}$ (in the UV−vis absorbance spectrum) for the substituted oxidized enzymes (pH 6.5 or 8.0) exhibit one major exponential decay, indicating the transfer of the hydride from NADPH to the flavin (Figure 6). The observed rate constant of flavin reduction is hyperbolically dependent on NADPH concentration (Figures 5 and 6), consistent with reversible formation of the charge-transfer complex prior to hydride transfer. The kinetics of reduction for all the substituted flavins is 2−15-fold faster at pH 8.0 than at pH 6.5 (Table 2).

PHBH reconstituted with 8-Cl-, 8-H-, and 8-$CH_3$-FAD (native flavin), analogues with relatively high redox potentials, shows three phases (in traces monitored at 690−750 nm) during the reduction reaction due to the formation and decay of a charge-transfer complex between reduced enzyme and oxidized pyridine nucleotide (8-X-$FADH^-$·$NADP^+$), which follows the initial formation of the NADPH·FAD charge-transfer complex (see above) (Figure 6A). This reduced enzyme-$NADP^+$ charge-transfer complex decays with a rate constant that is independent of the concentration of NADPH. Values for this decay ($k_3$) for enzyme forms containing flavins with −Cl, −H, and $-CH_3$ are 54.0, 40.5, and 25.0 $s^{-1}$ (pH 6.5) and 26.8, 17.6, and 18.0 $s^{-1}$ (pH 8.0). The intensity of the reduced flavin·$NADP^+$ charge-transfer absorbance band is dependent on the particular flavin used: 8-$CH_3 \approx$ 8-H < 8-Cl. Although on the basis of its high redox potential, 8-CN-FAD PHBH was expected to form a strong charge-transfer complex between reduced flavin and oxidized pyridine nucleotide, no indication of charge-transfer absorbance is observed during the reduction reaction (Figure 6B). The redox potential of 8-CN-FAD PHBH in the presence of *p*-OHB (+60 mV) is much higher than those of 8-Cl-FAD (−81 mV) and of native flavin (−163 mV). The inability to form good charge-transfer correlates with the reduction of 8-CN-FAD PHBH by NADPH being much slower than predicted from its redox potential (Table 2). The reduced flavin charge-transfer complex ($FADH^-$·$NADP^+$) is not

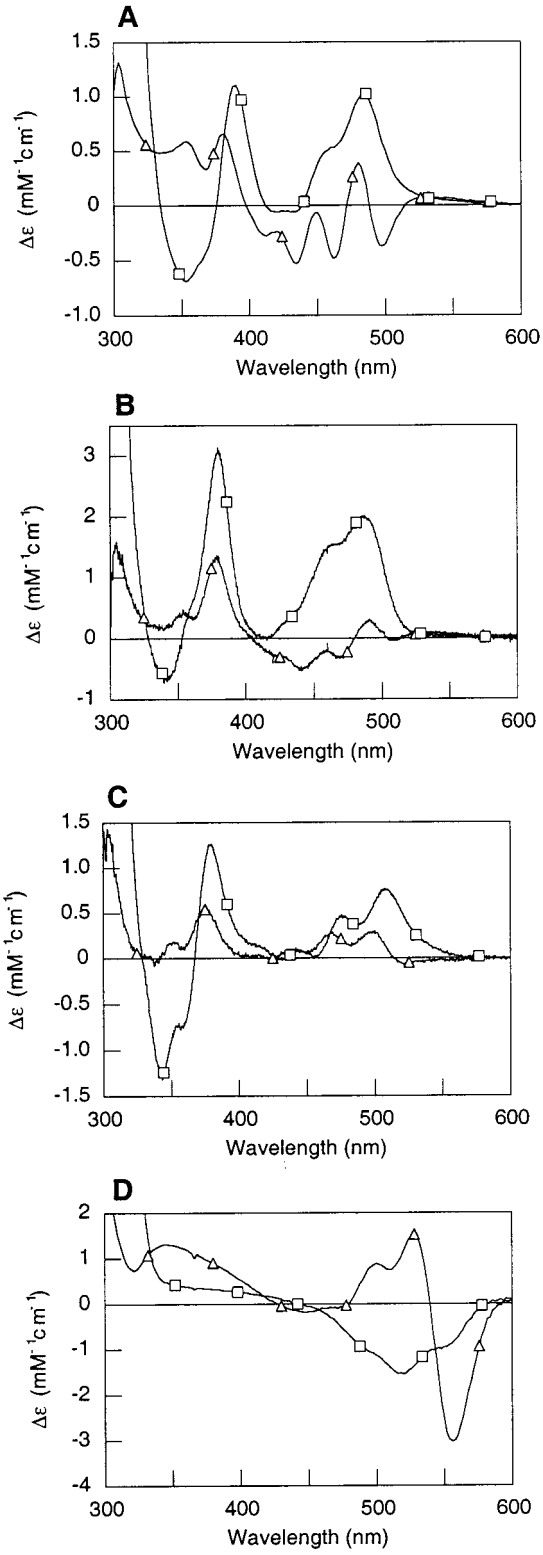


FIGURE 4: Absorption spectral perturbation of several 8-substituted PHBH upon ligand binding. Difference spectra are shown for substituted PHBH with the maximum concentration of *p*-OHB (△) and 2,4-DOHB (□) used. (A) 8-Cl-FAD, (B) 8-H-FAD, (C) 8-CN-FAD, and (D) 8-N$(CH_3)_2$-FAD PHBH. Dissociation constants (*24*) were determined by titrating ligand to enzyme ($\sim$30 $\mu$M) in 50 mM $KP_i$ and 1 mM EDTA, pH 6.5, at 4 °C and are reported in Table 2. Absorbance spectra were recorded, corrected for dilution, and the difference spectra obtained by subtracting the free enzyme spectrum from all successive spectra.

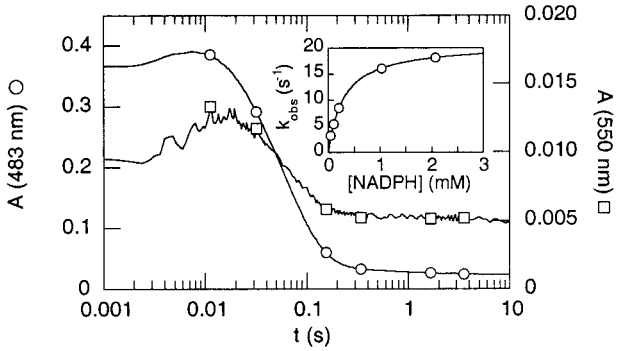


FIGURE 5: Kinetic traces from the reductive half reaction of 8-$SCH_3$-FAD PHBH in the presence of p-OHB. Anaerobic PHBH (15 $\mu$M) with bound *p*-OHB (0.5 mM) in 0.1 M Tris-sulfate (pH 8.0) was reacted with 2 mM NADPH at 4 °C in the same buffer solution using a stopped-flow spectrophotometer. Absorbance traces at indicated wavelengths are shown.

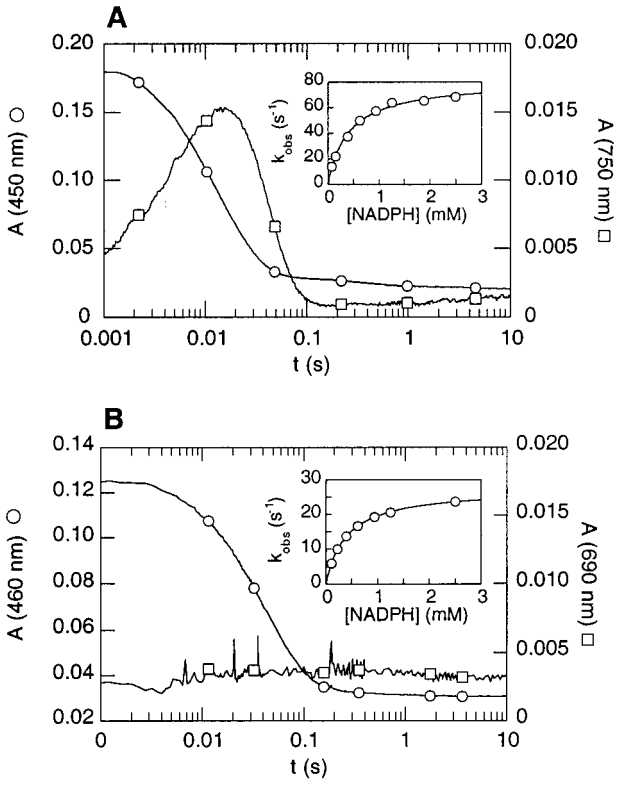


FIGURE 6: Kinetic traces from the reductive half reaction of (A) 8-Cl- and (B) 8-CN-FAD PHBH in the presence of p-OHB. Anaerobic enzyme (15 $\mu$M) with bound *p*-OHB (0.5 mM) in 50 mM $KP_i$ (pH 6.5) was reacted with 2.5 mM NADPH at 4 °C in the same buffer solution using a stopped-flow spectrophotometer. Absorbance traces at indicated wavelengths are shown.

observed when PHBH is reconstituted with low potential flavins (i.e., 8-$SCH_3$-, 8-$NH_2$-, 8-$N(CH_3)_2$-, 8-hydroxy-, and 8-mercapto-FAD), presumably because the rate constants for reduction by NADPH are smaller than the rate constants for dissociation of $NADP^+$ from the reduced enzyme (Table 2). Most of the dissociation constants for the binding of NADPH are similar to that for enzyme reconstituted with native flavin, either at pH 6.5 or 8.0 (Table 2). PHBH reconstituted with 8-$N(CH_3)_2$-, 8-hydroxy-, and 8-mercapto-FAD are the only examples that have appreciably larger dissociation constants for the binding of NADPH (Table 2). The reduction reactions of each of the enzymes, detected at the UV−vis absorbance maxima for the oxidized form of the flavin analogue, show

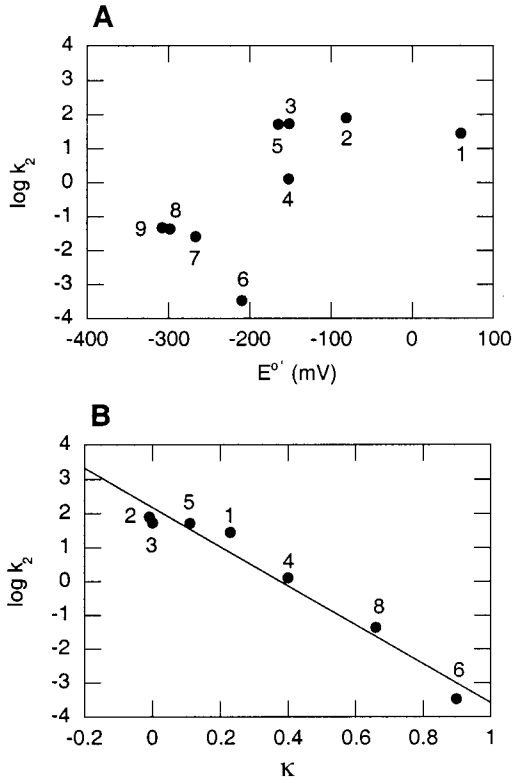


FIGURE 7: Free-energy relationship of the rate constants for NADPH reducing PHBH reconstituted with 8-substituted flavins. The log of the pseudo-first-order rate constants ($k_2$) for the hydride-transfer step are plotted vs (A) the $E^{o\prime}$ for the 8-substituted FAD bound to PHBH in the presence of *p*-OHB, and (B) the $\kappa$ substituent constant for the 8-substituent [$\kappa$ values are not available for 8-hydroxy ($O^-$) and 8-mercapto ($S^-$) substituents]. The reactions were carried out in KPi (pH 6.5) at 4 °C. The rates for 8-$N(CH_3)_2$-FAD enzyme were too slow to allow determination at 4 °C. Values were determined at 25 °C (Table 2) and decreased by a factor of 6 to allow for comparison with the other enzyme forms. This factor was obtained by comparison of rate constants at pH 8.0 for the two temperatures. See Table 4 for identification of the flavins.

a slow third phase with very small absorbance change; this might be attributed to the association of reduced enzyme with NADPH, but this was not investigated.

The rate constant for reduction ($k_2$, Scheme 1) of PHBH variants by NADPH is expected to correlate with the two-electron redox potential of the enzyme-bound flavin in the presence of *p*-OHB (*37*). However, a plot of redox potential as a function of the log $k_2$ (eq 1) shows poor correlation,

$$\log k_2 = \rho x + b \qquad (1)$$

even when 8-$N(CH_3)_2$-FAD, which is the largest flavin studied, is omitted from the analysis (Figure 7A) [log $k_2$ = $0.011E^{o\prime}$ (mV) + 1.824; $R = 0.656$, $F = 5.3$, with all data; log $k_2$ = $0.010E^{o\prime}$ (mV) + 2.016; $R = 0.787$, $F = 9.8$, omitting the data for 8-$N(CH_3)_2$-FAD]. In the case of 8-$N(CH_3)_2$-FAD PHBH [data point (**6**) in Figure 7A], the rate constant of reduction is much smaller (we measured 0.0014 $s^{-1}$ at 25 °C; using a factor of 6, we calculate a value of 0.000 23 $s^{-1}$ at 4 °C) than would be predicted from the redox potential alone. This unexpected behavior of 8-$N(CH_3)_2$-FAD may be due to steric effects of the substituent retarding the movement of the flavin into the appropriate conformation for reduction to take place. The poor correlation between the redox potential and the rate constant of reduction

Table 4: Substituent Constants[a]

| | 8-substituent | $\sigma_p$ | MR | $\pi$ | $\kappa$ |
|---|---|---|---|---|---|
| 1 | CN | 0.66 | 0.63 | na[b] | 0.23 |
| 2 | Cl | 0.23 | 0.60 | 0.71 | −0.01 |
| 3 | H | 0.0 | 0.10 | 0.00 | 0.00 |
| 4 | $SCH_3$ | 0.0 | 1.38 | 0.61 | 0.40 |
| 5 | $CH_3$ | −0.17 | 0.56 | 0.56 | 0.11 |
| 6 | $N(CH_3)_2$ | −0.83 | 1.55 | 0.18 | 0.90 |
| 7 | $S^-$ | −1.21 | na[b] | na[b] | na[b] |
| 8 | $NH_2$ | −0.66 | 0.54 | −1.23 | 0.66 |
| 9 | $O^-$ | −0.81 | na[b] | −3.87 | na[b] |

[a] Substituent constants are from ref *39*. [b] na = values not available.

Table 5: Dissociation and Reduction Rate Constants of PHBH Reconstituted With Several 8-Substituted Flavins by NADH[a]

| 8-substituent | $K_d$ ($\mu$M) | $k_2$ ($s^{-1}$) |
|---|---|---|
| CN | 1450 | 2.02 |
| Cl | 3300 | 2.19 |
| $CH_3$ | 5400 | 0.53 |
| $NH_2$ | 10 100 | 0.0075 |

[a] Dissociation constant for NADH and reduction rate constants were calculated from the kinetics of reduction of enzyme complexed with *p*-OHB determined in 50 mM $KP_i$ buffer (pH 6.5) at 4 °C. Values of rate constants were the average of at least four determinations. Rate constants varied ≤5 $\mu$M from one another.

indicates that factors other than chemical reactivity are involved during the reduction step (e.g., the lack of formation of a charge-transfer complex or adequate FAD conformational changes during the reduction process).

If the flavin needs to move to the out-conformation for reduction to take place, any factor such as a large 8-substituent that impedes this movement could diminish the rate of reduction. Alternatively, a large 8-substituent could sterically prevent the nicotinamide ring from approaching the flavin properly for hydride transfer. Thus, large substituents could account for the rate of reduction not correlating with the redox potential of the enzyme-bound flavin. The charge-transfer substituent constant ($\kappa$), determined by Foster et al. using NMR techniques (*38*), depends on the size and hydrophobicity of the proton donor and acceptor in charge-transfer complexes. Substitution into eq 1 with the substituent constant $\kappa$ for $x$ results in a linear relationship: $\log k_2 = -5.877\kappa + 2.194$; $R = 0.977$, $F = 104$ at pH 6.5 (Figure 7B). A similar correlation was obtained for the reaction performed at pH 8.0 ($\log k_2 = -5.378\kappa + 2.674$; $R = 0.971$, $F = 83$, see Tables 2 and 4). Since the charge-transfer constants ($\kappa$) for the substituents used in this study are strongly dependent on their size (MR) and hydrophobicity ($\pi$) ($\kappa = -0.367\pi + 0.601\text{MR} - 0.080$; $R = 0.975$, $F = 29$), it follows that a good correlation of $\log k_2$ with these parameters can also be obtained ($\log k_2 = 1.988\pi - 3.460\text{MR} + 2.529$; $R = 0.936$, $F = 11$). A multiregression analysis including the redox potential does not improve the fit [$\log k_2 = 0.003E^{\circ\prime}$ (mV) $+ 1.739\pi - 3.342\text{MR} + 2.918$; $R = 0.936$, $F = 4.8$], emphasizing the minor importance of the redox potential to the rate constant for reduction of the flavin.

*Reduction of the Different Enzyme Forms by Dihydronicotinamide Analogues*. Another approach for understanding the possible importance of flavin position and rate of reduction of the enzyme-bound flavin was to measure the rate constants for reduction of the PHBH-substituted flavins by pyridine nucleotide analogues with different sizes of the pyridinium side chain (Scheme 2, e.g., NADH, NMNH, and NMeH). This could test whether smaller reduced pyridines would be less impeded by the bulkier 8-substituents of the flavins. To probe the importance of the R group of the nicotinamide analogues in the reduction reaction, PHBH variants reconstituted with 8-substituted flavins and complexed with *p*-OHB were reduced with 1 mM to 15 mM NADH or NMeH, or 1 mM to 50 mM NMNH. Traces recorded at UV−vis absorbance maxima for reduction of the oxidized enzyme forms showed a monophasic decay for the reduction reaction with NADH, NMNH, and NMeH. The observed rate constants for the exponential decay are dependent on the pyridine nucleotide concentration and are about 16-fold (pH 6.5) to 95-fold (pH 8.0) smaller than that for NADPH (see Table 2 for $k_2$ by NMeH, see below for $k_2$ by NMNH, and see Table 5 for $k_2$ by NADH).

Rate constants for reduction by NADH of PHBH reconstituted with different 8-substituted flavins and in complex with *p*-OHB at pH 6.5 also show poor correlation with the two-electron redox potential of PHBH variants ($\log k_2 = 0.007E^{\circ\prime} + 0.381$; $R = 0.877$, $F = 6.7$) (Table 5). Using the substituent constant $\kappa$ to correlate the rate of reduction of the different PHBH flavin forms by NADH gave a significantly better relationship ($\log k_2 = -3.633\kappa + 0.462$; $R = 0.916$, $F = 11$), analogous to behavior observed for reduction by NADPH. Binding of NADH to the modified enzymes was 4−160-fold weaker than binding of NADPH (see Tables 2 and 5).

Because of its poor reactivity and poor binding to the enzyme, reduction of PHBH by NMNH was carried out only at pH 6.5 with enzyme containing native FAD. NMNH interacts very weakly with the enzyme ($K_d \approx 53$ mM); the dissociation constant for NMNH binding to native PHBH is ∼250-fold weaker than binding of NADPH and ∼14-fold weaker than binding of NADH or NMeH. The rate constant for reduction of native PHBH by NMNH is 0.48 $s^{-1}$, similar to the rate constant for reduction of this enzyme by NADH ($k_2 = 0.53$ $s^{-1}$).

Reduction of the enzymes with NMeH was carried out in 0.1 M Tris-$SO_4$ buffer (pH 8.0) because in $KP_i$ buffer (pH 6.5) this nicotinamide analogue decomposes rapidly. Traces recorded at the UV−vis absorbance maxima for the oxidized enzymes exhibit a decrease in the initial absorbance that occurs within the dead-time of the stopped-flow instrument. This decrease of the initial absorbance corresponds to the formation of the oxidized flavin·NMeH charge-transfer complex. By contrast, enzyme reconstituted with 8-$SCH_3$-FAD shows a small increase in absorbance at 483 nm ($\lambda_{max}$ of the UV−vis spectrum for oxidized enzyme) before 10 ms ($k_1 \approx 5 \times 10^5$ $M^{-1}$ $s^{-1}$), similar to that previously observed during reduction of this enzyme form by NADPH, but with less change in absorbance. Following this initial fast step, an exponential decay is observed. Enzyme reconstituted with flavins having −Cl, −H, and $-CH_3$ substituents at the 8-position show a small increase followed by a decrease in absorbance at 550 nm, indicating the formation and decay of the initial charge-transfer complex between oxidized flavin and NMeH (data not shown). The observed rate constant for the reduction of the enzyme-bound flavin by NMeH is hyperbolically dependent on NMeH concentra-

tion, permitting the calculation of $K_d$-values. PHBH reconstituted with 8-substituted flavins formed complexes with NMeH with values of dissociation constants similar to that of native enzyme (Table 2). The reduction rate constant for NMeH correlated better than with NADPH with the redox potential of the enzyme-bound flavins ($\log k_2 = 0.009E^{\circ\prime}$ (mV) + 1.861; $R = 0.829$, $F = 11$) but not as well with the substituent constant $\kappa$ ($\log k_2 = -3.044\kappa + 1.536$; $R = 0.849$, $F = 13$) (Figure 8). However, the combination of the two constants gives a high correlation ($\log k_2 = 0.006E^{\circ\prime}$ (mV) $- 2.035\kappa + 2.043$; $R = 0.958$, $F = 22$) (Figure 8C). After reduction of the flavin analogues, no charge-transfer between reduced flavin ($FADH^-$) and oxidized nicotinamide ($NMe^+$) was observed; presumably the decay for the reduced flavin charge-transfer complex was too fast to allow accumulation of the intermediate.

## DISCUSSION

The results presented here are consistent with the hypothesis of Palfey et al. (*18*) that the flavin in PHBH should move to the out-conformation for proper reduction by NADPH (Figure 1). We have shown on the basis of spectral perturbations (Figure 4) that PHBH reconstituted with any of several different flavin analogues is able to acquire either flavin conformation (in or out) depending upon which ligand binds. Furthermore, binding of *p*-OHB to enzyme that has been reconstituted with any of the flavin analogues does not affect the redox potential of the enzyme-bound flavin, except with the case of 8-CN-FAD. The redox potential of PHBH reconstituted with 8-CN-FAD increased 23 mV upon binding substrate (ref *24* and Table 2). The affinity of 8-CN-FAD PHBH for *p*-OHB can therefore be expected to be at least 10-fold higher for its reduced form than for the oxidized enzyme.

Although the rate constant for reduction of PHBH reconstituted with 8-substituted flavins by NADPH (at pH 6.5 or pH 8.0) was expected to correlate with the 2-electron redox potential of the enzyme-bound flavin according to eq 1, poor correlation was observed. However, the rate constants correlated well with the substituent constant $\kappa$, which is based on size and hydrophobicity of the 8-substituent on the flavin. Substitution of the methyl group at the 8-position of the flavin by larger groups, e.g., $-N(CH_3)_2$, decreases the rate of flavin reduction much more than would be expected on the basis of the redox potential of the enzyme-bound flavins. This behavior might be accounted if the larger 8-substituents (1) impeded the movement of the flavin to the out-conformation, (2) prevented the nicotinamide from gaining access to the active site to reduce the flavin located in the in-conformation, or (3) prevented the optimal interaction for hydride transfer in the transition state. In contrast to nicotinamide nucleotides, the rate of reduction of PHBH reconstituted with 8-substituted flavins by NMeH does depend significantly on the redox potential of the flavin, implying that movement of the flavin to the out-position is not such a critical factor with this small dihydronicotinamide as it is with the bulky NADPH. Moreover, because reduction by the smaller nicotinamides is slower, the impeded movement of the flavin due to the 8-substituents may not be as rate determining. Alternatively, the smaller nicotinamides may not require the flavin to completely move to the out-position for reduction to occur.

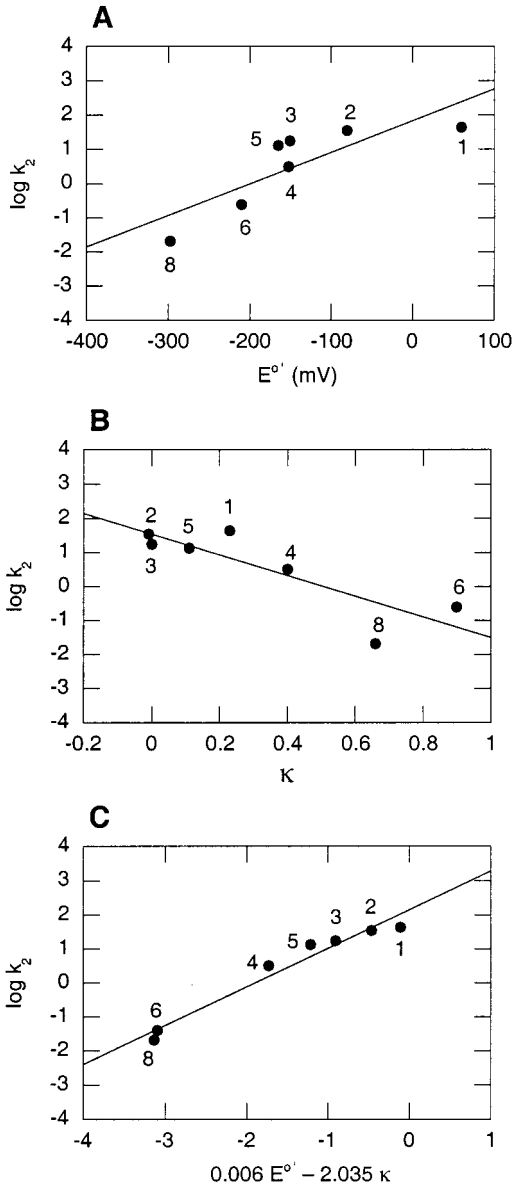


FIGURE 8: Free-energy relationship of the rate constants for NMeH reducing PHBH reconstituted with 8-substituted flavins. The log of the pseudo-first-order rate constants ($k_2$) for the hydride-transfer step is plotted vs (A) the $E^{\circ\prime}$ for the 8-substituted FAD bound to PHBH in the presence of *p*-OHB, (B) the $\kappa$ substituent constant for the 8-substituent, and (C) a combination of $\kappa$ and redox potential. The reactions were carried out in Tris-sulfate (pH 8.0) at 4 °C. See Table 2 for identification of the flavins.

The angle and distance between hydride donor and acceptor have been shown to be critical for the hydride-transfer reactions catalyzed by isocitrate dehydrogenase (*40*) and dihydrofolate reductase (*41*), as well as in semiempirical quantum chemical calculations and ab initio calculations for hydride transfer (*41*, *42*). The optimal distance for hydride transfer between C4 of the nicotinamide and N5 of the flavin for glutathione reductase has been calculated to be 2.67 Å (*42*). The modeled distance (energy minimized) for PHBH with the FAD in the out-position is 3.9 Å (*23*). Thus, some movement is likely to be required to form the charge-transfer complex prior to hydride transfer. Marcus theory (*43*) can explain how both the alteration in the redox potential of the FAD analogues and the disturbed orientation of reactants prior to hydride-transfer can influence the rate of reduction

of enzyme-bound flavin. Marcus theory postulates that the activation energy of a reaction is expressed by two or more components, an intrinsic thermodynamic barrier (dependent on the redox potential of the reactants, FAD and NADPH, in the hydride-transfer complex) and the work component implicated in bringing the reactants and products together in the proper orientation, as has been proposed for PHBH (*11*). Results presented here are consistent with the work component being important because the rate constant for the reduction reaction of PHBH reconstituted with different 8-substituted flavin analogues is influenced by size and hydrophobicity of the substituent on the FAD.

The movement of the flavin to the out-position may be triggered by more than one factor. For example, the anionic 2′-phosphoryl group present in NADPH (p$K_a$ ~7.0) may contribute to this conformational change, since hydride-transfer to PHBH reconstituted with native flavin from NADH, NMNH, or NMeH is much slower than that by NADPH. The average rate constant of reduction is 0.6 $s^{-1}$ at pH 6.5 for NADH and NMNH and 11 $s^{-1}$ at pH 8.0 for NMeH compared to 52 $s^{-1}$ and 94 $s^{-1}$ at pH 6.5 and 8.0 for NADPH. Binding of these nicotinamide analogues to PHBH with native flavin is >12-fold weaker compared to binding of NADPH. Reduction of PHBH at pH 8.0 is faster than reduction measured at pH 6.5, possibly because there is an increased fraction of the anionic form of the substrate, *p*-OHB, which is known to be important during the oxidation reaction and recently associated with enhancement of the reduction step (*18*). Alternatively, it could be due to an increased fraction of the anionic 2′-phosphoryl group in NADPH that is essential for enzyme recognition and for triggering the flavin movement. Removal of the 2′-phosphoryl group of NADPH leads to a loss of 1.4 kcal $mol^{-1}$ of ground-state binding energy in PHBH containing FAD (eq 2).

$$\Delta\Delta G = -RT \ln\left(\frac{K_d^{NADPH}}{K_d^{NADH}}\right) \qquad (2)$$

The rate-limiting step in catalysis for native enzyme in the presence of *p*-OHB at pH 6.5 might be determined by both the conformational change (movement of the FAD to the out-position) required for ligand to be exchanged (*14*) and the dehydration of the flavin-C4a-hydroxide to form oxidized flavin (steps indicated by $k_6$ and $k_7$ in Scheme 1). Modification at the 8-position of the FAD can affect which of the steps are rate limiting in PHBH catalysis (*24*). For example, the rate of turnover ($k_{cat}$) by PHBH reconstituted with 8-Cl-FAD, calculated from the individual rate constants under saturating conditions of substrate and cofactor (pH 6.5, 4 °C), suggests that $k_{cat}$ is determined both by the off rate of $NADP^+$ and the release of the hydroxylated product ($k_3$ and $k_7$ of Scheme 1). The mechanism of Scheme 1 using the individual rate constants predicts a value for $k_{cat} = k_2k_3k_5k_7/(k_3k_5k_7 + k_2k_5k_7 + k_2k_3k_5)$. The constants $k_2$, $k_3$, $k_5$, and $k_7$ are 80, 54, 300, and 45 $s^{-1}$. From these values, a value for $k_{cat}$ of 18 $s^{-1}$ is predicted. However, the experimentally determined $k_{cat}$ for PHBH reconstituted with 8-Cl-FAD with *p*-OHB as a substrate is 11 $s^{-1}$. This suggests that there is a spectrally silent step of about 30 $s^{-1}$ that could be related to flavin movement during the reaction.

This study has demonstrated that the redox potentials of the reactive chemical species are not the only factors driving the redox chemistry. Multiple properties of the enzyme, such as proper conformation of the prosthetic group, its redox potential, electrostatics in the cavity of the active site, nature of active-site residues, and the size and/or hydrophobicity of the substituents used (either in the flavin or the nicotinamide) are all important for catalysis.

## ACKNOWLEDGMENT

We thank Drs. Barrie Entsch and Graham R. Moran for providing the pIE-130 plasmid and Dr. Bruce A. Palfey for scientific advice.

## REFERENCES

1. Scopes, R. K. (1978) *Eur. J. Biochem. 85*, 503−516.
2. Bernstein, B. E., and Hol, W. G. (1998) *Biochemistry 37*, 4429−4436.
3. Wilkinson K. D. Rose I. A. (1979) *J. Biol. Chem. 254*, 12567−12572.
4. Entsch, B., Ballou, D. P., and Massey, V. (1976) *J. Biol. Chem. 251*, 2550−2563.
5. Entsch, B., Massey, V., and Ballou, D. P. (1974) *Biochem. Biophys. Res. Commun. 57*, 1018−1025.
6. Entsch, B., and Ballou, D. P. (1989) *Biochim. Biophys. Acta 999*, 313−322.
7. Spector, T., and Massey, V. (1972) *J. Biol. Chem. 247*, 4679−4687.
8. van Berkel, W. J., Eppink, M. H., and Schreuder, H. A. (1994) *Protein Sci. 3*, 2245−2253.
9. Lah, M. S., Palfey, B. A., Schreuder, H. A., and Ludwig, M. L. (1994) *Biochemistry 33*, 1555−1564.
10. Gatti, D. L., Entsch, B., Ballou, D. P., and Ludwig, M. L. (1996) *Biochemistry 35*, 567−578.
11. Palfey, B. A., Entsch, B., Ballou, D. P., and Massey, V. (1994) *Biochemistry 33*, 1545−1554.
12. Moran, G. R., Entsch, B., Palfey, B. A., and Ballou, D. P. (1997) *Biochemistry 36*, 7548−7556.
13. Moran, G. R., Entsch, B., Palfey, B. A., and Ballou, D. P. (1996) *Biochemistry 35*, 9278−9285.
14. Gatti, D. L., Palfey, B. A., Lah, M. S., Entsch, B., Massey, V., Ballou, D. P., and Ludwig, M. L. (1994) *Science 266*, 110−114.
15. Schreuder, H. A., Mattevi, A., Obmolova, G., Kalk, K. H., Hol, W. G., van der Bolt, F. J., and van Berkel, W. J. (1994) *Biochemistry 33*, 10161−10170.
16. van der Bolt, F. J., Vervoort, J., and van Berkel, W. J. (1996) *Eur. J. Biochem. 237*, 592−600.
17. Palfey, B. A., Ballou, D. P., and Massey, V. (1997) *Biochemistry 36*, 15713−15723.
18. Palfey, B. A., Moran, G. R., Entsch, B., Ballou, D. P., and Massey, V. (1999) *Biochemistry 38*, 1153−1158.
19. Schreuder, H. A., Hol, W. G., and Drenth, J. (1990) *Biochemistry 29*, 3101−3108.
20. Enroth, C., Neujahr, H., Schneider, G., and Lindqvist, Y. (1998) *Structure 6*, 605−617.
21. Manstein, D. J., Pai, E. F., Schopfer, L. M., and Massey, V. (1986) *Biochemistry 25*, 6807−6816.
22. Ryerson, C. C., Ballou, D. P., and Walsh, C. (1982) *Biochemistry 21*, 1144−1151.
23. Eppink, M. H., Schreuder, H. A., and van Berkel, W. J. (1998) *J. Biol. Chem. 273*, 21031−21039.
24. Ortiz-Maldonado, M., Ballou, D. P., and Massey, V. (1999) *Biochemistry 38*, 8124−8137.
25. Spencer, R., Fisher, J., and Walsh, C. (1976) *Biochemistry 15*, 1043−1053.
26. Entsch, B., Palfey, B. A., Ballou, D. P., and Massey, V. (1991) *J. Biol. Chem. 266*, 17341−17349.
27. Muller, F., and van Berkel, W. J. (1982) *Eur. J. Biochem. 128*, 21−27.

28. Massey, V. (1990) in *Flavins and Flavoproteins* (Curti, B., Ronchi, S., and Zanetti, G., Eds.) pp 59−66, Walter de Gruyter and Co., Berlin.
29. van der Laan, J. M., Swarte, M. B. A., Groedijk, H., Hol, W. G. J., and Drenth, J. (1989) *Eur. J. Biochem. 179*, 715−724.
30. Brunger, A. T., Adams, P. D., Clore, G. M., DeLano, W. L., Gros, P., Grosse-Kunstleve, R. W., Jiang, J. S., Kuszewski, J., Nilges, M., Pannu, N. S., Read, R. J., Rice, L. M., Simonson, T., and Warren, G. L. (1998) *Acta Crystallogr., Sect. D 54*, 905−921.
31. Adams, P. D., Pannu, N. S, Read, R. J., and Brunger, A. T. (1997) *Proc. Natl. Acad. Sci. U.S.A. 94*, 5018−5023.
32. McRee, D. E. (1992) *J. Mol. Graphics 10*, 44−46.
33. Suelter, C. H., and Metzler, D. E. (1960) *Biochim. Biophys. Acta 44*, 23−33.
34. Bevington, P. R. (1969) *Data Reduction and Error Analysis for the Physical Sciences*, McGraw-Hill, Inc., New York.
35. McRee, D. E. (1999) *J. Struct. Biol. 125*, 156−165.
36. Schopfer, L. M., Massey, V., and Claiborne, A. (1981) *J. Biol. Chem. 256*, 7329−7337.
37. Light D. R., and Walsh C. (1980) *J. Biol. Chem. 255*, 4264−4277.
38. Foster, R., Hyde, R. M., and Livingstone, D. J. (1978) *J. Pharm. Sci. 67*, 1310−1313.
39. Hansch, C., and Leo, A. (1995) *Exploring QSAR: Hydrophobic, Electronic, and Steric Constants*, ACS Professional Reference Book, American Chemical Society, Washington DC.
40. Mesecar, A. D., Stoddard, B. L., and Koshland, D. E. Jr. (1997) *Science 277*, 202−206.
41. Benkovic, S. J., Fierke, C. A., and Naylor, A. M. (1988) *Science 239*, 1105−1110.
42. Mestres, J., Duran, M., and Bertran, J. (1996) *Bioorg. Chem. 24*, 69−80.
43. Sühnel J., and Schowen, R. L. (1991) in *Enzyme mechanism from isotope effects* (Cook, P. F., Ed.) pp 3−35, CRC Press, Inc., Boca Raton.
44. Read, R. J. (1986) *Acta Crystallogr., Sect. A 42*, 140−149.

BI991603U